

1 **Adaptive plasticity in the healthy reading network investigated through combined**
2 **neurostimulation and neuroimaging**

3 Turker, S.¹, Kuhnke, P.^{1,2}, Schmid, F. R.³, Cheung, V. K. M.⁴, Zeidler, B.⁵, Seidel, K.¹, Eckert,
4 L.¹, & G. Hartwigsen¹

5 ¹ Lise Meitner Research Group ‘Cognition and Plasticity’, Max Planck Institute for Human
6 Cognitive and Brain Sciences, Leipzig, Germany

7 ² Wilhelm Wundt Institute for Psychology, University of Leipzig, Germany

8 ³ CBC Center for Brain and Cognition, Universitat Pompeu Fabra, Barcelona

9 ⁴ Institute of Information Science, Academia Sinica, Taipei, Taiwan

10 ⁵ Centre for Systematic Musicology, University of Graz, Austria

11 **Abstract (199 words).** The reading network in the human brain comprises several regions,
12 including the left inferior frontal cortex (IFC), ventral occipito-temporal cortex (vOTC) and dorsal
13 temporo-parietal cortex (TPC). The left TPC is crucial for phonological decoding, i.e., for learning
14 and retaining sound-letter mappings. Here, we tested the causal contribution of this area for reading
15 with repetitive transcranial magnetic stimulation (rTMS) and explored the response of the reading
16 network using functional magnetic resonance imaging (fMRI). 28 healthy adult readers overtly
17 read simple and complex words and pseudowords during fMRI after effective or sham TMS over
18 the left TPC. Behaviorally, effective stimulation slowed pseudoword reading. A multivariate
19 pattern analysis showed a shift in activity patterns in the left IFC for pseudoword reading after
20 effective relative to sham TMS. Furthermore, active TMS led to increased effective connectivity
21 from the left vOTC to the left TPC, specifically for pseudoword processing. The observed changes
22 in task-related activity and connectivity suggest compensatory reorganization in the reading
23 network following TMS-induced disruption of the left TPC. Our findings provide first evidence
24 for a causal role of the left TPC for overt pseudoword reading and emphasize the relevance of
25 functional interactions in the healthy reading network for successful pseudoword processing.

26

27 **1. Introduction**

28 Reading is a core feature of human communication and crucial for participating in everyday social
29 life, work and interpersonal communication. Fluent reading is based upon multiple, hierarchically
30 organized processes, including orthographic recognition, orthographic-phonological mapping (i.e.,
31 decoding), and semantic access (Xia et al., 2017). Known words, regardless their complexity, are
32 usually automatically accessed as whole word forms in the mental lexicon (so-called sight word
33 reading) (Ehri, 2005). Reading this sentence took you probably only a few seconds although you
34 had to process the pronunciation and meaning of eighteen words consecutively and at a high speed.
35 The single sounds that make up these words were most likely beyond your awareness, i.e., you did
36 not have to look at single letters or decode them for reading the sentence. When reading
37 pseudowords (i.e., words without any meaning), on the other hand, you rely considerably on the
38 single sounds and/or the syllables they occur in. Therefore, reading (complex) pseudowords is
39 more challenging for typical adult readers because it is a non-automatic reading process.

40 The universal reading network in the human brain supporting these processes comprises
41 three major circuits: (i) the left inferior frontal cortex (IFC), (ii) the left dorsal temporo-parietal
42 cortex (TPC) and (iii) the left ventral occipito-temporal cortex (vOTC) (Pugh et al., 2001; Rueckl
43 et al., 2015). Neuroimaging studies suggest that the left IFC is involved in various processes,
44 including attention and language functions (e.g., phonological output resolution; Taylor et al.,
45 2013). The left TPC, often referred to as the ‘decoding’ center in the human brain, is responsible
46 for the transformation of orthographic elements into associated phonological codes (Linkersdörfer
47 et al., 2012). The last region, the left vOTC, shows growing sensitivity to print during reading
48 acquisition (Chyl et al., 2021) and optimizes linguistic processing for quick access to familiar
49 words by filtering out meaningless grapheme strings (e.g., pseudowords) (Gagl et al., 2020).

50 Although non-invasive brain stimulation (NIBS) studies have proliferated over the past
51 two decades, only few studies have applied NIBS to specifically modulate reading-related
52 processes, and practically none have explored the effect of NIBS on overt pseudoword reading
53 (Turker & Hartwigsen, 2021a). Understanding the causal engagement and functional contribution
54 of brain areas to reading, however, is vital to improve our understanding of the healthy reading
55 network. Additionally, it can help uncover and alleviate potential deficits encountered by
56 individuals with dyslexia (see Turker & Hartwigsen, 2021b). Existing NIBS studies with typical

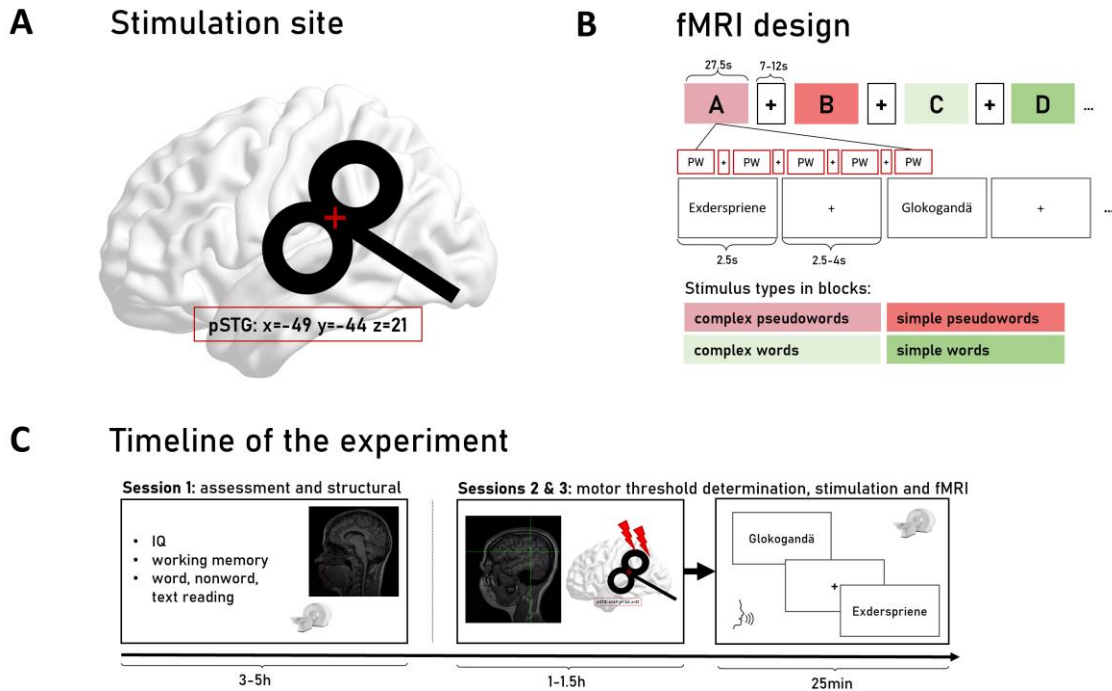
57 readers provide first evidence for causal roles of reading-related regions to different reading
58 subprocesses (see summary in Turker & Hartwigsen, 2021a). For instance, the left anterior and
59 posterior IFC contribute to phonological and semantic aspects of reading, respectively (e.g., Devlin
60 et al., 2003; Gough et al., 2005; Hartwigsen et al., 2010 a,b). Other studies further highlight the
61 left vOTC as critical region for word processing (Duncan et al., 2010) but also confirm its
62 relevance for pseudoword processing (Pattamadilok et al., 2015). Finally, the left TPC was
63 identified as key area for phonological processes related to reading, in line with its expected role
64 as grapheme-phoneme-conversion center (e.g., Costanzo et al., 2012; Liederman et al., 2003).
65 However, existing NIBS studies on pseudoword reading focused on relatively simple bisyllabic
66 pseudowords and included few trials. Moreover, none of the previous studies used neuroimaging
67 to explore the underlying neuronal changes induced by neurostimulation. Consequently, the
68 underlying neural correlates of stimulation-induced modulation of the reading network remain
69 unclear.

70 Likewise, NIBS studies with atypical readers support the causal role of the left TPC to
71 reading, but neglect underlying neural changes and mechanisms (see review by Turker &
72 Hartwigsen, 2021b). Behaviorally, several single- or multiple-session studies with individuals with
73 dyslexia found NIBS-induced improvements in reading performance in low frequency word,
74 pseudoword and text reading after facilitation of the left TPC, or simultaneous inhibition of the
75 right TPC and facilitation of the left TPC (e.g., Costanzo et al., 2016, 2019; Lazzaro et al., 2020,
76 2021). This further supports the critical role of the left TPC for reading processing but leaves open
77 questions regarding potential NIBS-induced changes on the neural level, such as the potential of
78 NIBS to modify the reading network transiently or permanently.

79 What are the neural correlates of the observed NIBS-induced behavioral modulation of
80 reading performance in typical and atypical readers? On the one hand, facilitatory and inhibitory
81 NIBS most likely either in- or decrease functional brain activation in the targeted area, which
82 should in turn map onto changes in behavioral performance (Miniussi et al., 2013). Since
83 individuals with dyslexia across all age groups show less engagement of the left TPC during
84 reading when compared to typical readers (Richlan et al., 2011, 2013; Turker, 2018), it seems
85 likely that inhibitory NIBS should result in a deterioration of reading performance in typical
86 readers, whereas facilitation should help improve reading skills in atypical readers. On the other

87 hand, impairing a core node of a network most likely results in significant up- and down-
88 regulations in tightly connected brain regions, both in terms of functional activation and
89 connectivity (Sale et al., 2015). Such potential compensatory mechanisms should occur after
90 disruption of the targeted area, as described in previous combined TMS-fMRI studies in the
91 language network and may be correlated with changes in behavioral performance (see Hartwigsen
92 et al., 2013; Hartwigsen et al., 2017). Indeed, neuroimaging suggests that phonological deficits in
93 children with dyslexia could stem from a disruption of functional connectivity between the three
94 core reading areas (left IFC, vOTC and TPC) (van der Mark et al., 2011; Schurz et al., 2015),
95 highlighting the importance of considering within-network-interaction. In terms of reading, it
96 remains yet to be explored whether NIBS can alter functional activation and connectivity within
97 the reading network, and whether this directly maps onto reading performance.

98 In the present study, we tested: (i) the causal contribution of the left TPC for efficient word
99 and pseudoword reading by inducing a focal perturbation with repetitive transcranial magnetic
100 stimulation (rTMS); and (ii) explore the reading network's response to perturbation in terms of
101 functional activation and connectivity. We hypothesized that the inhibition of the left TPC would
102 lead to an increase in reading times and a decrease in accuracy for simple and complex
103 pseudowords, with a stronger effect on complex pseudowords. Our second hypothesis was that the
104 disruption of the left TPC should lead to an up-regulation of the left IFC and vOTC (i.e., higher
105 activation within these areas and higher functional coupling with the disrupted region), and
106 potentially also the contralateral right TPC (see Hartwigsen & Volz, 2021). This would be in line
107 with our hypotheses that a disruption of the reading circuit requires functional reorganization and
108 compensatory mechanisms to sustain reading. To test these hypotheses, we applied offline
109 effective or sham rTMS to the left TPC of healthy adults who then performed a reading task during
110 functional MRI. Subjects were asked to read aloud easy and complex words and pseudowords (see
111 **Figure 1**). As main findings, we observed that effective rTMS (relative to sham stimulation) led
112 to (1) slower speech onsets for pseudowords, (2) a shift in task-related activation patterns in the
113 left IFC during pseudoword reading, and (3) stronger task-related functional coupling between the
114 left vOTC and the left TPC.



115

Figure 1 Details on stimulation site (A), fMRI design (B) and timeline of the experiment (C). The target was chosen based on previous meta-analyses and was situated in the left pSTG (-49/-44/21). During fMRI, subjects read simple and complex words and pseudowords (200 trials per scanning session; total duration: ~25 minutes).

116 2. Results

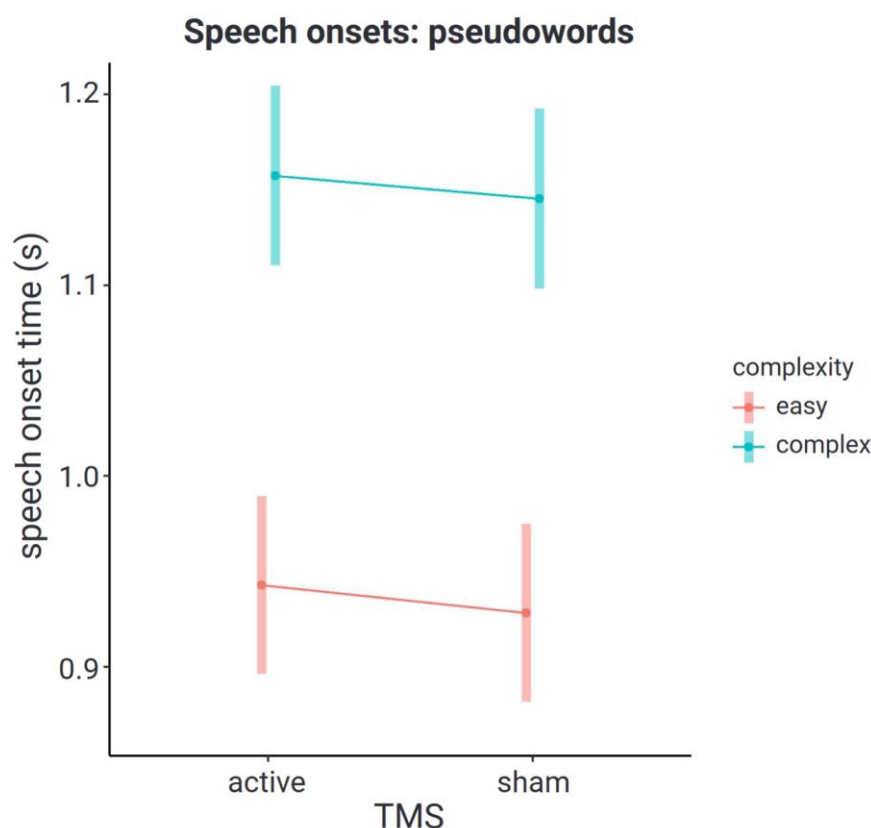
117

118 2.1. Behavioral findings

119 We modelled the speech onset and accuracy of each trial using generalized linear mixed models
120 (Tables 1-3). As fixed effects, the interaction between TMS (effective vs. sham), complexity
121 (simple vs. complex stimuli), and stimulus type (words vs. pseudowords) and lower order terms
122 were included in the model. A maximal random effects structure was used for each model to guard
123 against inflated Type I errors. Results for speech onsets are displayed in **Tables 1 and 2** and
124 visualized in **Figure 2**, results for reading accuracy are provided in **Table 3**.

125 The model shows that participants generally showed significantly longer speech onset
126 times for pseudowords compared to words and for complex compared to simple stimuli. Likewise,
127 subjects showed lower accuracy for pseudoword as compared to word reading. Significant
128 complexity-by-pseudoword interactions furthermore indicated that these effects were enhanced for
129 complex pseudowords. As for TMS effects, we found a marginally significant TMS-by-

130 pseudoword interaction ($p=0.051$) for speech onsets (**Table 1**). Step-down analyses (**Table 2**)
 131 suggest that the effect was driven by a delay of 13 – 16 ms in pseudoword reading. Interestingly,
 132 the TMS effect on pseudowords was significant when the model included random intercepts
 133 ($p=0.035$), but not anymore when we included random slopes. This suggests large inter-individual
 134 variability in TMS response, which makes effects that generalize to the population hard to detect.
 135 We did not find any effect of TMS on reading accuracy (**Table 3**).



136

Figure 2 TMS effect on pseudoword speech onsets (active stimulation vs. sham stimulation) modelled by word complexity (0 = simple; 1= complex)

137 **Table 1** Effects of TMS on speech onsets. Speech onsets of each trial were modelled to follow a
 138 Gamma distribution using a generalized linear mixed model. Significance of predictors were
 139 assessed using the Wald test. *: $p < 0.05$, **: $p < 0.01$, ***: $p < 0.001$

Predictor	$\chi^2(1)$	p-value
Intercept	1614.6620	$< 2.20 \times 10^{-16}$ ***
TMS	0.0039	0.950
Complexity	64.2319	1.11×10^{-15} ***

Pseudoword	148.9187	$< 2.20 \times 10^{-16}$ ***
TMS x Complexity	1.9935	0.158
TMS x Pseudoword	3.7938	0.051
Complexity x Pseudoword	42.2177	8.17×10^{-11} ***
TMS x Complexity x Pseudoword	0.8281	0.363

140 **Table 2** Marginal effect of TMS (effective – sham) on speech onsets for pseudowords using step-
 141 down analysis. Models with random subject intercepts and with or without random slopes for TMS
 142 were fitted. Significance predictors were assessed using the Wald test. *: $p < 0.05$, **: $p < 0.01$,
 143 ***: $p < 0.001$

Condition	Mean TMS effect (ms)	SEM (ms)	z-score	p-value
Without TMS random slope				
Word	8.31	4.61	1.80	0.072
Pseudoword	13.07	6.19	2.11	0.035 *
With TMS random slope				
Word	5.34	16.67	0.32	0.749
Pseudoword	16.25	17.24	0.94	0.346

144 **Table 3** Effects of TMS on response accuracy. Correct and incorrect responses of each trial were
 145 modelled using a binomial generalized linear mixed model. Significance predictors were assessed
 146 using the Wald test. *: $p < 0.05$, **: $p < 0.01$, ***: $p < 0.001$

Predictor	$\chi^2(1)$	p-value
Intercept	128.4377	$< 2.20 \times 10^{-16}$ ***
TMS	0.0020	0.964
Complexity	0.2867	0.592
Pseudoword	18.9644	1.33×10^{-5} ***
TMS x Complexity	0.0034	0.953
TMS x Pseudoword	0.0290	0.865
Complexity x Pseudoword	5.6493	0.017 *
TMS: Complexity x Pseudoword	0.0671	0.796

147

148 2.2. Functional activation

149 To explore differences in reading processing for stimulus type and complexity, we performed
 150 within-session univariate whole-brain analyses of the sham condition (see **Figure 3**). Pseudowords
 151 (bi- and four-syllabic) activated the left motor cortex, the left IFC, the bilateral posterior parietal
 152 cortices and the bilateral vOTC more than words. While activation of the motor cortex is most
 153 likely tied to higher articulation demands, the engagement of the other areas seems to be related to

154 higher reading demands as compared to word processing. Words, on the other hand, led to higher
155 activation in brain areas corresponding to the default mode network (DMN) (Smallwood et al.,
156 2021). These include the bilateral angular gyri, middle temporal gyri, middle frontal cortices, and
157 bilateral medial brain regions including the medial prefrontal cortices and the posteromedial
158 cortices. Since sight word reading is an automatized, higher-order cognitive task, it is little
159 surprising that word reading recruits areas of the DMN more strongly than pseudoword reading.
160 Especially since word reading is reliant upon lexical retrieval and semantic access, which are
161 known to depend on processing in the left angular gyrus and the left middle temporal cortex to left
162 anterior temporal lobe. Recently, the role of the posterior parietal cortex for reading was confirmed
163 in a few NIBS studies (Turker & Hartwigsen, 2021a for review). A stronger engagement of the
164 visual word form area and its homologue for pseudoword processing, on the other hand, have not
165 been explicitly discussed in research to date. Regarding complexity, we find primarily higher
166 activation for complex stimuli in the bilateral motor cortices, the bilateral superior temporal gyri
167 and areas within the posterior parietal cortex and occipital lobes.

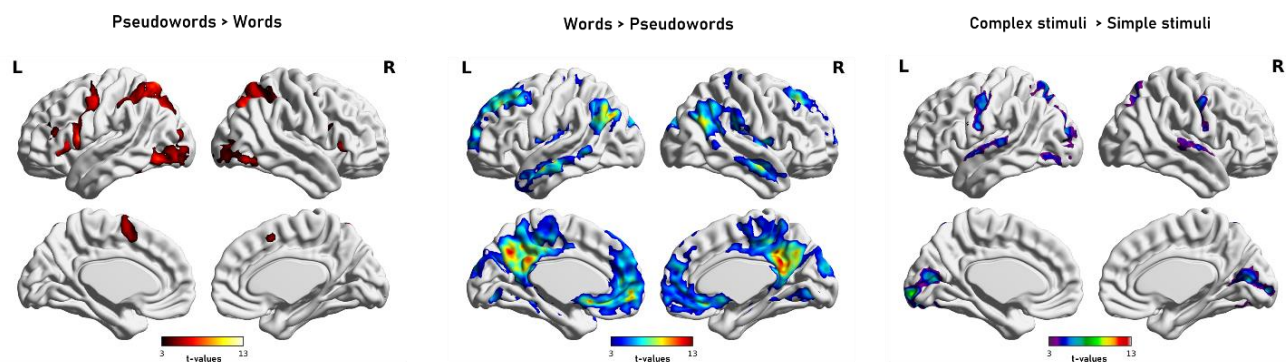
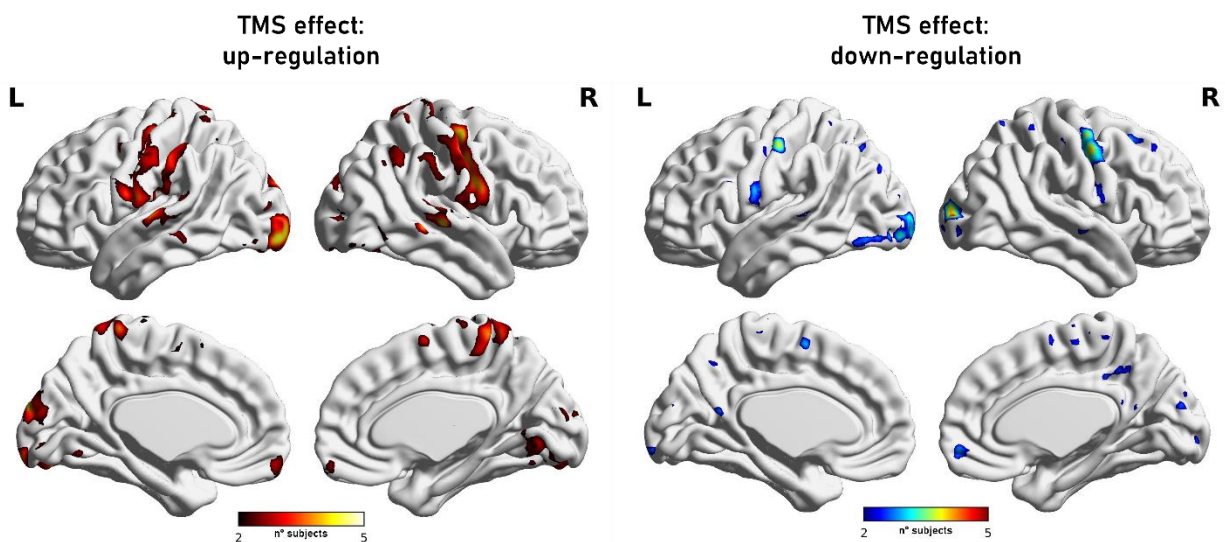


Figure 3 *Univariate contrast maps.* Results show functional brain activation differences due to stimulus type (pseudowords vs. words) and complexity ((complex pseudowords + complex words) > (simple pseudowords + simple words)) corrected at $p < 0.001$ voxel-level and FWE-cluster-corrected at $p < 0.05$.

168 Regarding TMS effects, univariate whole-brain analyses showed no significant differences
169 in brain activation when comparing effective and sham TMS, not even for complex pseudowords
170 that have the highest decoding demand. To better understand this, we performed an exploratory
171 subject-specific analysis with individual subject maps thresholded at $p < .001$ (uncorrected) (**Figure**
172 **4**). Supporting our observation of large inter-individual variability in behavioral response to TMS,
173 participants also showed large differences in univariate brain activation involving up- and down-

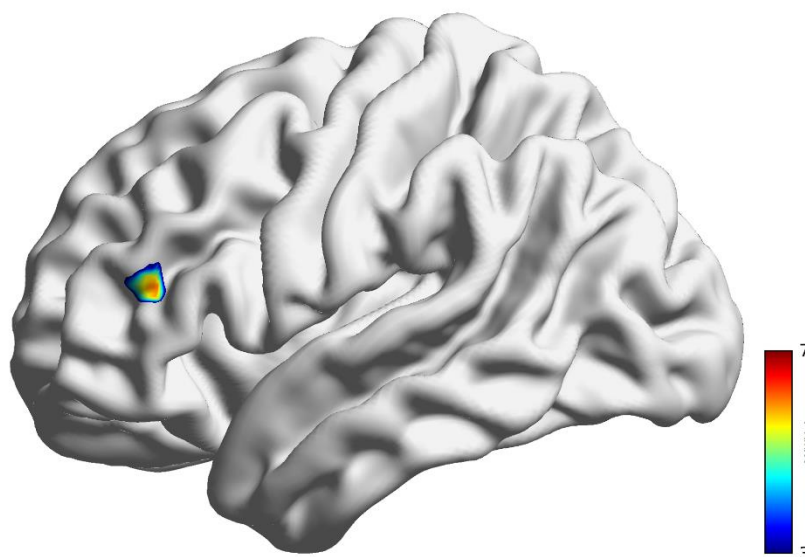
174 regulation of the bilateral motor cortices and the occipital lobe bilaterally following effective TMS.
175 It is particularly striking that the increased and decreased activation in response to effective TMS
176 comprises largely overlapping areas in these regions. In other words, some individuals responded
177 with more and others with less activation in the bilateral motor areas, portions of the superior
178 temporal gyrus, and occipital areas in response to effective TMS as compared to sham TMS. These
179 preliminary analyses show that neural responses to TMS differ considerably between individuals,
180 which might explain the lack of group-level differences.



181 **Figure 4.** *Exploratory individual subject maps of functional activation in response to effective TMS as compared to sham. Results on the left side show an up-regulation, i.e., a higher activation in brain areas after effective stimulation. Results on the right side show areas that responded to effective TMS with a down-regulation, i.e., with less brain activation. ($p < 0.001$ uncorrected at the voxel level thresholded at 2 subjects; colour indicates number of subjects showing increase/decrease in the same voxel).*

182 Since univariate analyses are often claimed to be insensitive to fine-grained differences in
183 multi-voxel activity patterns we additionally performed a multivariate pattern analysis (MVPA) to
184 investigate the effect of TMS on functional activation patterns within the core reading areas.
185 Specifically, we used a spherical 5-mm “searchlight” across the whole brain, and at each
186 searchlight location, we trained a machine learning classifier to decode between effective and sham
187 TMS across participants, separately for words and pseudowords. We found above-chance
188 between-subject decoding in the left posterior IFC selectively for pseudowords (**Figure 5**) (see a
189 discussion on the role of the left mid to posterior IFC for pseudoword processing in Turkur &

190 Hartwigsen, 2021b). No effects were observed for word processing, supporting our hypothesis that
191 effective stimulation of the left TPC primarily influences pseudoword processing. These findings
192 indicate that effective TMS over the left TPC altered fine-grained multi-voxel activity patterns for
193 pseudoword reading in the left IFG (pars triangularis) by resulting in a shift of the task-related
194 activity pattern in that area.



195

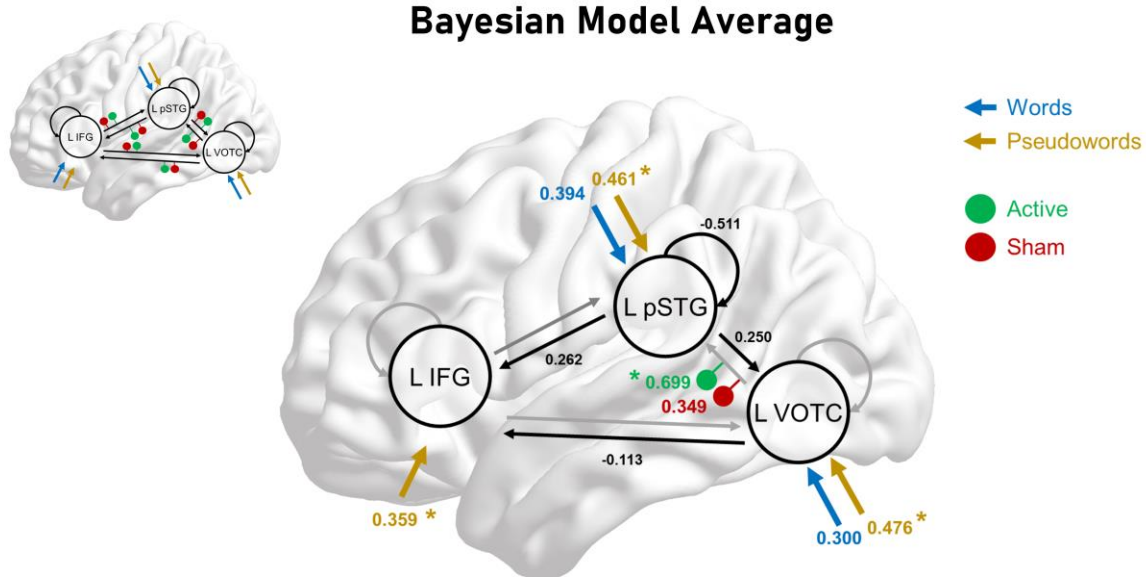
Figure 5 Results for between-subject searchlight MVPA. Following effective stimulation of the left TPC as compared to sham stimulation, we find a shift in functional activation patterns in the left IFG selectively for pseudoword reading. Activity patterns comprised beta estimates for each mini-block (see **Figure 1**) of every participant.

196 **2.3. Effective connectivity**

197 Finally, we performed Dynamic Causal Modeling (DCM) to map TMS-induced changes in
198 effective connectivity within the reading network. The DCM model included the core reading areas
199 (the left IFG, the left vOTC and the left TPC) that represent core nodes of the reading network that
200 were also active for pseudoword and word reading, independent of TMS. We performed a DCM
201 group analysis using Bayesian Model Reduction (Friston et al., 2016; Zeidman et al., 2019 a,b).
202 To this end, we first defined a ‘full’ DCM model for each subject. According to this model, all
203 three areas were bidirectionally connected, words and pseudowords could serve as driving inputs

204 to every region, and each between-region connection could be modulated by effective and sham
205 TMS. Bayesian Model Reduction then compared this full model to numerous reduced models.
206 Finally, we computed the Bayesian model average, which is the average of parameter values across
207 models weighted by each model's probability, and thresholded the BMA at 99% parameter
208 probability (see **Figure 6**).

"Full" DCM Model (for Bayesian Model Reduction)



209 **Figure 6** *Dynamic causal modeling results.* *Left: The "full" DCM model that served as starting
210 point for Bayesian model reduction. Black arrows represent intrinsic connections, coloured arrows
211 denote driving inputs, and coloured dots represent modulatory inputs. Right:
212 The resulting Bayesian Model Average thresholded at 99% parameter probability. Driving and
213 between-region parameters are in units of Hz. Modulatory parameters in- or decrease connections
214 in an additive manner. *: Significantly stronger modulation than other parameters ($P_p > 0.99$).
215
216

217 We found strong evidence for intrinsic connectivity within all three areas and pseudowords
218 drove all three regions more strongly than words (Bayesian contrasts for TPC: $P_p=0.999$; IFG:
219 $P_p=1.0$; vOTC: $P_p=1.0$). Crucially, effective connectivity from the left vOTC to the left TPC was
220 significantly increased by effective TMS over the left TPC (modulation: 0.699; result: 0.464 Hz).
221 This modulation was much stronger for effective than for sham TMS (modulation: 0.349; result:
222 0.113 Hz; Bayesian contrast between active and sham TMS: $P_p=1.0$). In other words, a disruption
223 of the left TPC resulted in a stronger facilitatory drive from the left vOTC to the left TPC, which
224 can be interpreted as a compensatory mechanism (see Discussion).

3. Discussion

225 *The role of the left TPC for pseudoword reading*

226 In our present study, we explored whether the left TPC, a critical region for acquiring and
227 establishing sound-letter mappings, is causally involved in pseudoword processing in adult
228 readers. In other words, we tested if the typically reading brain still relies on this brain region when
229 confronted with a task that requires access to singles sounds and syllables. Our findings show that
230 a disruption of the left TPC impacts pseudoword processing. An inhibition of this area with TMS
231 led to an increase of speech onsets for pseudowords. These behavioral changes were underpinned
232 by a modulation of task-related activity and connectivity in the larger network for reading, likely
233 reflecting compensatory reorganization in the reading network which may have helped to maintain
234 processing. While the absence of a TMS-induced modulation of task-related activation in the
235 stimulated area may be surprising, previous work demonstrated compensatory reorganization in
236 distributed networks after inhibitory TMS for language and other cognitive tasks (see Hartwigsen
237 & Volz, 2021 for review). Moreover, the behavioral relevance of remote changes induced by TMS
238 in the language network has also been shown (Hartwigsen et al., 2017).

239 Although our findings support earlier TMS studies reporting NIBS-induced deteriorations
240 or improvements in phonological performance (Turker & Hartwigsen, 2021 a, b), our study is the
241 first to provide direct evidence for a significant role of the left TPC for overt simple and complex
242 pseudoword reading. The only comparable previous behavioral TMS study targeting the left TPC
243 (Costanzo et al., 2012) reported an increase in reading accuracy but no differences in speech onsets.
244 While facilitatory TMS effects on task performance are often interpreted as causal evidence for
245 the contribution of the targeted area to a given task, such effects could also reflect the inhibition
246 of task-irrelevant areas that compete for resources (Luber & Lisanby, 2014; see Bergmann &
247 Hartwigsen, 2021 for discussion). The difference in the direction of results in the previous and
248 present study is unclear. We believe that these differences could stem from a more precise
249 neuronavigation in the present study, which may have resulted in targeting a different (sub-)region
250 in our study, more complex stimuli (four instead of two or three syllables), a larger sample size
251 and differences in stimulation parameters (continuous theta burst stimulation/cTBS instead of
252 high-frequency rTMS). One other study tested pseudoword reading following TMS but in this
253 language mapping study by Hauck and colleagues (2015a, b) several regions were targeted but no
254 strong effect of TMS on the TPC could be found for pseudoword reading. Consequently, we here

255 provide first evidence that the left TPC is causally involved in pseudoword processing since
256 inhibitory TMS led to slower pseudoword reading and modulated communication within the
257 reading network.

258 The observed TMS effect confirms neuroimaging findings indicating that the left
259 TPC/inferior parietal cortex is still involved in spelling-sound conversion in adults (Taylor et al.,
260 2013), despite evidence of this area's contribution to various tasks including verbal working
261 memory (Jonides et al., 1998) and executive processing (Binder et al., 2005). However, it also
262 stands a bit in contrast to a meta-analysis on reading processing in child- and adulthood by Martin
263 et al. (2015), who reported a strong engagement of the left TPC in children, but no significant
264 activation in that area across neuroimaging studies with adults. Notably, the disruptive TMS effect
265 of the present study was significant for pseudowords only (although words showed a trend towards
266 delayed speech onsets). This observation may point to the relevance of the left TPC for
267 phonological processing during reading. Alternatively, the stronger effect on pseudoword reading
268 may have resulted from increased task difficulty for pseudoword relative to word reading. The
269 behavioral results further showed a strong interaction between complexity and pseudowords, but
270 this effect did not interact with TMS. Therefore, it is unlikely that the observed effect can
271 selectively be explained by general task complexity.

272 Why would we see differences in speech onsets and not reading times? Even when asked
273 to read written stimuli overtly, we process them before we start actual speech production, that is,
274 as soon as we see them, we process and thus read them (we are unable to “not read” visual stimuli).
275 Therefore, inhibiting an area that is crucial for access to letter-sound knowledge, will more likely
276 impair this inner, ‘silent’ reading process than the task of speech production, which relies heavily
277 on motor areas (Brown et al., 2005) and does not reflect reading mechanisms per se.

278 *Adaptive plasticity within the reading network*

279 The present study is the first study that mapped TMS-induced behavioral changes on reading
280 performance on the neural level with fMRI. Earlier research on language skills more generally
281 suggests that TMS leads to plastic after-effects, such as large-scale changes on the network level
282 affecting both local and remote activity within targeted networks, as well as interactions between
283 other involved networks (Hartwigsen & Volz, 2021). As such, the perturbed brain can flexibly
284 redistribute and functionally reorganize its computational capacities to compensate for the

285 disruption of an area or the network. The present study adds first evidence for compensatory
286 mechanisms within the typical reading network in terms of functional brain activation. We did not
287 detect any significant TMS-related differences with univariate measures of brain activation,
288 probably due to the observed strong interindividual variability in response to stimulation, which
289 has already been reported for motor excitability in previous studies (see Hamada et al., 2013).

290 Nevertheless, we found TMS-induced changes in fine-grained multi-voxel activity patterns
291 in the left IFC between effective and sham TMS, selectively for pseudoword (but not for word)
292 reading. In terms of the functional role of the left IFC for reading, theories hold that it is crucial
293 for phonological output resolution and rhyming during reading (Taylor et al., 2013; Brozdowski
294 & Booth, 2021), as well as attention and working memory (Corbetta et al., 2002; Tops & Boksem,
295 2011). With pseudowords having a higher decoding demand and thus requiring more effort,
296 specifically after inhibition of the left TPC, it is likely that differences in response patterns of the
297 left IFC at least partially stem from higher demands on attention, executive functions, and
298 cognitive control. Alternatively, the stronger contribution of left IFC to pseudoword reading after
299 disruption of the left TPC might also reflect a shift in the balance towards another key node for
300 reading, and thus reflect phonological processes per se. This explanation would be in line with
301 previous TMS studies showing flexible redistribution between homologous areas (e.g., Hartwigsen
302 et al., 2013; Jung & Lambon Ralph, 2016) or remote regions from the same specialized subnetwork
303 (Hallam et al., 2016) during different language tasks (e.g., Hartwigsen, 2016). A stronger
304 contribution of the left IFC after disruption of the left TPC likely reflects compensatory attempts
305 in the network which helped to maintain task processing at a high level and may have prevented
306 decreases in task accuracy.

307 Apart from the TMS-induced changes in response patterns, we found a shift in functional
308 coupling between the left vOTC and the left TPC in response to inhibition of the latter. After
309 effective TMS over the left TPC, as compared to sham stimulation, the left vOTC increased its
310 facilitatory drive onto the left TPC. This is particularly interesting since the left vOTC plays a key
311 role in orthographic processing and is vital for reading words and pseudowords (Jobard et al.,
312 2003, Turker & Hartwigsen, 2021a). A functional engagement of this region for pseudoword
313 processing could also be confirmed in the univariate analyses of this study. This observation of the
314 left vOTC exerting a stronger influence on the left TPC during pseudoword processing could be

315 interpreted as a compensatory mechanism. As such, functional connectivity between these two
316 areas is most likely vital for successful and efficient decoding, so that a disruption of the left TPC
317 requires an up-regulation of functional coupling to compensate for the increased demand posed by
318 the task. This highlights the importance of considering within-network interactions when exploring
319 TMS-induced effects on the neural level. When considering TMS-induced changes on task-related
320 activity and connectivity, it is important to bear in mind that TMS is not “lesioning” an area and
321 unlikely to completely “silence” processing in the targeted region. Consequently, a shift in the
322 balance between different nodes in the respective network with a stronger contribution of another
323 area may help to maintain processing at a relatively high level, despite the disruption (see
324 Hartwigsen, 2018).

325 Overall, the present study emphasizes the relevance of the three core reading areas for
326 pseudoword reading. It seems that the targeted region, the left TPC, is crucial for pseudoword
327 processing, most likely for the processing of very complex stimuli. However, the reading network
328 in typical adult readers is flexible enough to adapt to the disruption by increasing functional
329 coupling between the left vOTC and the left TPC, and at the same time shifting functional brain
330 activation in the left IFC. Since we still see a slight deterioration in pseudoword reading
331 performance, as hypothesized, neural plasticity seems to be only partially successful at
332 accommodating the induced disruption. This might still explain why the effects were not as large
333 as expected, and only slightly affected response efficiency but not accuracy. The observed small
334 behavioral effects most likely stem from large inter-individual variability in response to TMS. It
335 seems that TMS responses are largely variable between individuals, which makes group-level
336 analyses particularly challenging and explains both the small behavioral effects and the lack of
337 univariate whole-brain activation differences in our study.

338 With respect to the contribution of our data to theoretical reading models, our study can be
339 explained under the framework of two reading models, one being the connectionist framework of
340 reading (Seidenberg et al., 2005), the other the dual-cascaded model of reading (DRC; Coltheart
341 et al., 2001). The findings do not provide evidence for a hierarchical organization of the reading
342 network, but they suggest a constant interaction between reading areas, more in line with
343 connectionist accounts. Furthermore, the findings highlight that decoding recruits the left TPC,
344 which is in line with earlier assumptions that unfamiliar word and pseudoword reading rely upon

345 a dorsal reading stream, including recruitment of the vOTC, the left TPC and the left IFC (backed
346 by structural connectivity research, e.g., Cummine et al., 2015). Since we did not observe any
347 effects on word processing, this suggests that words might recruit a different route that does not
348 require the left TPC. However, words could also be too automatized and robustly presented in the
349 semantic lexicon as to respond to a TMS-induced disruption in the left TPC.

350 **4. Conclusion**

351 The present study provides first evidence that the left TPC is causally involved in overt
352 pseudoword reading and confirms adaptive plasticity within the reading network. By combining
353 rTMS with fMRI, we found that effective disruption led to (1) slower reading of pseudowords,
354 manifested as a delay in speech onsets for simple and complex pseudowords, (2) a change in
355 functional activation patterns in the left IFC as revealed by MVPA, and (3) an increase of
356 functional coupling between the left vOTC and the left TPC. The latter two can be interpreted as
357 compensatory mechanisms that show adaptive plasticity in the reading network in response to
358 perturbation.

359 In summary, we report neurophysiological changes in response to TMS at the level of task-
360 related activity and connectivity in addition to generally confirming earlier findings on causal
361 contributions of the left TPC to reading-related phonological processes (e.g., Liederman et al.,
362 2003; Costanzo et al., 2012). Even though we only used a single session intervention in this study,
363 we could still see immediate effects on the behavioral and neural levels. The present findings can
364 guide future studies and suggest new perspectives concerning the treatment of reading disorders,
365 e.g., by designing multiple-session interventions for individuals with reading impairments.
366 Overall, our study advances future experimental and translational applications of TMS in health
367 and disease.

368

369

370 **5. Methods**

371 **5.1. Participants**

372 Participants were young, healthy, right-handed adults (N = 28; 13 females; range: 18-40 years,
373 $M_{\text{age}}=25\pm 4$) with no prior history of psychiatric, neurological, hearing, or developmental disorders.
374 All participants had nonverbal intelligence scores within the normal range or above (nonverbal IQ:
375 ≥ 91 ; CFT 20-R; Weiß, 2019). Sample size was determined based on comparable previous TMS
376 studies (e.g., Kuhnke et al., 2020). Participants were either recruited via the participants database
377 of the Max Planck Institute for Human Cognitive and Brain Sciences Leipzig (MPI CBS), or flyers,
378 posters, and social media. Participation in all sessions was required for the respective participant's
379 data to be included in the study sample. Prior to participation, written informed consent was
380 obtained from each subject. The study was performed according to the guidelines of the
381 Declaration of Helsinki and approved by the local ethics committee of the University of Leipzig.

382 In accordance with the given governmental regulations and measures regarding the
383 COVID-19 pandemic, participants were not allowed to have been to risk areas two weeks prior to
384 study participation and were required to undergo a SARS-CoV-2 rapid antigen self-test upon
385 arrival provided by the MPI CBS. Further, subjects were requested to sign a form stating that, in
386 case of a positive result of the self-test, participation in the study had to be suspended.

387 **5.2. Experimental procedure and behavioral reading assessment**

388 The present study comprised one 3-hour behavioral testing session and two combined fMRI-TMS
389 sessions (one for each TMS condition). During the behavioral testing session, we assessed
390 nonverbal intelligence, working memory, and reading. However, for the present analysis, we only
391 made sure that participants had normal nonverbal intelligence, reading and working memory. The
392 *Culture Fair Test* (CFT 20-R; Weiß, 2019) was administered to test participants' nonverbal
393 intelligence. Verbal working memory was measured through digit span forward and digit span
394 backward taken from the *Wechsler Adult Intelligence Scale* (WAIS-I; Petermann & Petermann,
395 2011). Additionally, nonword span (Mottier Test in the ZLT II- Zürcher Lesetest; Petermann &
396 Daseking, 2019) was assessed. The test was terminated if the subject could not repeat 50% of
397 syllables in one trial block. Silent text reading was assessed with the LGVT 5–12+ (Schneider et

398 al., 2017), providing speed (number of words read), accuracy (ratio of filled gaps and correct items)
399 and comprehension scores (number of correctly inserted words).

400 The TMS-fMRI sessions were separated by at least 7 days to prevent carry-over effects of
401 TMS, and session order (sham or effective) was counterbalanced across participants. The study
402 employed a 2x2x2 within-subject design with the factors TMS (effective stimulation, sham
403 stimulation), stimulus type (words, pseudowords) and complexity (simple stimuli consisting of
404 two syllables, complex stimuli consisting of four syllables) (for details of the experimental
405 procedure, stimulation site and fMRI design, see **Figure 1**).

406 **5.3. Transcranial magnetic stimulation (TMS)**

407 To investigate the causal role of the left TPC for phonological processing, we applied “offline”
408 (i.e, before the task) continuous theta burst stimulation (cTBS). cTBS applies bursts of 3 stimuli
409 at 50 Hz repeated at intervals of 200 ms (5 Hz) for 40 seconds (total: 600 pulses) (Huang et al.,
410 2005). Offline protocols can induce adaptive changes in brain activity and connectivity that outlast
411 the stimulation for up to 60 minutes (Siebner & Rothwell, 2003). Participants underwent one
412 effective and one sham (placebo) session. The sham condition mirrored the effective condition in
413 terms of basic set-up and procedure, but a placebo coil (MCF-P-B65) was used, which features the
414 same mechanical outline and acoustic noise as the effective coil but reduces the magnetic field
415 strength by ~80%.

416 Intensity of the stimulation was set at 90% of the individual resting motor threshold (rMT)
417 The protocol for assessing the resting motor threshold was conducted in accordance with the
418 standardized procedure proposed by Schutter and van Honk (2006). This procedure applies
419 electromyography instead of purely visual observation of muscle twitch. rMT was determined as
420 the lowest stimulation intensity producing at least 5 motor evoked potentials of $\geq 50 \mu\text{V}$ in the
421 relaxed first dorsal interosseus muscle of the right hand when single-pulse TMS was applied over
422 the hand region of left primary motor cortex 10 times.

423 The specific MNI coordinates for the left TPC ($x=-49$, $y=-44$, $z=21$) were calculated from
424 three meta-analyses on reading impairments (Maisog et al., 2008; Richlan et al. 2009, 2011). To
425 precisely target these coordinates in each individual participant, they were transformed from MNI
426 to subject space using the *SPM12* software (Wellcome Trust Center for Neuroimaging, University
427 College London, UK). We then used stereotactic neuronavigation (TMS Navigator, Localite

428 GmbH, Sankt Augustin, Germany) to navigate the coil over the target area and maintain its location
429 throughout stimulation. For neuronavigation, participants' heads were co-registered onto their T1-
430 weighted MR image before the stimulation sessions. T1 scans were obtained beforehand with a 3T
431 MRI scanner (Siemens, Erlangen, Germany) using an MPRAGE sequence (176 slices in sagittal
432 orientation; repetition time: 2.3 s; echo time: 2.98 ms; field of view: 256 mm; voxel size: 1 x 1 x
433 1 mm; no slice gap; flip angle: 9°; phase encoding direction: A/P).

434 **5.4. Functional neuroimaging**

435 *Stimuli*

436 We used an event-related mini-block design that used 400 stimuli altogether (200 simple and
437 complex words; 200 simple and complex pseudowords). In each session, participants read
438 randomly chosen 100 words (50 simple, 50 complex) and 100 pseudowords (50 simple, 50
439 complex) in mini-blocks (5 stimuli presented after another) aloud in the scanner (i.e., stimuli were
440 not repeated in the second session to avoid remembering pseudowords). The 200 simple word
441 stimuli consisted of two syllables and 4-6 letters and were taken from Schuster et al. (2015). As
442 complex words, we chose the first 100 most frequent 4-syllabic words (10-14 letters) from the dlex
443 database (<http://www.dlexdb.de/>). We excluded compound words and plurals but due to the small
444 number of available complex words we had to include a few 3-syllabic words and plurals (in
445 German the plural is usually constructed by adding a whole syllable). Pseudowords were then
446 designed using Wuggy (<http://crr.ugent.be/programs-data/wuggy>) based on the simple and
447 complex word lists. We excluded pseudowords that were too similar to real German words (<2
448 letters difference).

449 **Neuroimaging**

450 Functional MRI data were collected on a 3T Siemens Magnetom Skyra scanner (Siemens,
451 Erlangen, Germany) with a 32-channel head coil. Blood oxygenation level-dependent (BOLD)
452 images were acquired with a single-echo BOLD EPI sequence (repetition time [TR]: 2s, echo time
453 [TE]: 22ms; flip angle: 80°; field of view [FoV]: 204 mm; voxel size: 2.5 x 2.5 x 2.5 mm;
454 bandwidth: 1794 Hz/Px; phase encoding direction: A/P; acceleration factor: 3). B0 field maps were
455 acquired for susceptibility distortion correction using a spin-echo BOLD EPI sequence (TR:
456 8000ms; TE:50ms; flip angle: 90°; bandwidth: 1794 Hz/Px).

457 During fMRI, stimuli were presented for 2.5 seconds. We jittered the between-stimulus-
458 interval, as well as the between-mini-block-interval. Each block lasted for 27.5 seconds and
459 participants were in the scanner for around 25 minutes (see **Figure 1**). Subjects were instructed to
460 read out all stimuli as fast and correct as they could with as little head movement as possible.
461 Subjects' in-scanner responses were recorded and manually preprocessed with audacity. Speech
462 on- and offsets were determined with Praat by four independent raters, two analyzing each
463 audiofile in 50% of cases. We computed an interrater reliability >0.85 suggesting that
464 determination of speech on- and offsets was very similar between raters. For the following
465 analyses, we averaged speech onsets across raters if they were rated by more than one person.
466 Accuracy for all trials was checked by a third person.

467 **5.5. Data analysis**

468 **5.5.1. Linear Mixed Model**

469 Speech onsets and response accuracy of each trial were analysed with generalised linear mixed
470 models (GLMM) using glmmTMB 1.1.2.3 (Brooks et al., 2017) in R 4.0.5. To circumvent the need
471 to transform reaction times to satisfy normality assumptions, reading times were modelled using a
472 Gamma distribution with the identity link function (Lo & Andrews, 2015). The accuracy of each
473 trial (correct versus incorrect) was modelled as a binary response using a binomial distribution and
474 logit link function. All models included as fixed effects the three-way interaction between TMS
475 (sham/active), Pseudoword (pseudoword/word), and Complexity (simple/complex), and all lower
476 order terms. A maximal random effects structure was used for all models with subject as the
477 grouping variable to avoid inflated Type I errors (Barr et al., 2013). The resulting GLMM for
478 speech onsets included random intercepts, and random slopes for the interaction between TMS,
479 Complexity and Pseudoword, as well as all lower order terms. Likewise, random intercepts and
480 random slopes for TMS and Complexity were included in the GLMM for response accuracy. The
481 significance of each variable was assessed using the Wald test, and marginal effects were
482 calculated using a step-down simple effects analysis.

483 **5.5.2. fMRI analysis**

484 *Preprocessing*

485 MRI preprocessing was performed using *fMRIPrep* (version 20.2.1; Esteban et al. 2019).
486 Anatomical T1-weighted images were corrected for intensity non-uniformity (using
487 *N4BiasFieldCorrection* from ANTs 2.3.3), skull-stripped (using *antsBrainExtraction* from ANTs
488 2.3.3), segmented into gray matter, white matter and cerebrospinal fluid (using *fast* in FSL 5.0.9),
489 and normalized to MNI space (MNI152NLin2009cAsym; using *antsRegistration* in ANTs 2.3.3).
490 Brain surfaces were reconstructed using *reconall* (FreeSurfer 6.0.1).

491 Functional BOLD images were co-registered to the anatomical image (using *bbregister* in
492 FreeSurfer 6.0.1), distortion corrected based on B0-fieldmaps (using *3dQwarp* in AFNI
493 20160207), slice-timing corrected (using *3dTshift* from AFNI 20160207), motion corrected (using
494 *mcflirt* from FSL 5.0.9), normalized to MNI space (via the anatomical-to-MNI transformation),
495 and smoothed with a 5 mm³ FWHM Gaussian kernel (using *SPM12*; Wellcome Trust Centre for
496 Neuroimaging; <http://www.fil.ion.ucl.ac.uk/spm/>). Moreover, physiological noise regressors were
497 extracted using the anatomical version of *CompCor* (aCompCor, Behzadi et al., 2007).

498 *Univariate analyses*

499 We performed a whole-brain random-effects group analysis based on the general linear model
500 (GLM), using the two-level approach in *SPM12*. At the first level, individual participant data were
501 modeled separately. The participant-level GLM included regressors for the 4 experimental
502 conditions, modelling trials as box car functions (2.5 s duration) convolved with the canonical
503 HRF. Only correct trials were analyzed, error trials were modeled in a separate regressor-of-no-
504 interest. Nuisance regressors included 24 motion regressors (the 6 base motion parameters + 6
505 temporal derivatives of the motion parameters + 12 quadratic terms of the motion parameters and
506 their temporal derivatives), individual regressors for time points with strong volume-to-volume
507 movement (framewise displacement > 0.9; Siegel et al. 2014), and the top 10 aCompCor regressors
508 explaining the most variance in physiological noise. The data were subjected to an AR(1) auto-
509 correlation model to account for temporal auto-correlations, and high-pass filtered (cutoff 128 s)
510 to remove low-frequency noise.

511 Contrast images for each participant were computed at the first level. At the second level,
512 these contrast images were submitted to one-sample or paired t-tests (to test for interactions). For
513 all second-level analyses, a gray matter mask was applied, restricting statistical tests to voxels with
514 a gray matter probability > 0.1 (MNI152NLin2009cAsym gray matter template in *fMRIPrep*). All

515 activation maps were thresholded at a voxel-wise $p < 0.001$ and a cluster-wise $p < 0.05$ FWE-
516 corrected.

517 ***Multivariate pattern analysis (MVPA)***

518 As univariate analyses are insensitive to information represented in fine-grained, multi-voxel
519 activation patterns (Haxby et al., 2014), we additionally performed a multivariate pattern analysis
520 (MVPA) using *The Decoding Toolbox* (Hebart et al., 2015) implemented in *Matlab* (version
521 2021a). Our MVPA aimed to test whether effective TMS over TPC, as compared to sham TMS,
522 modulated activity patterns in the stimulated or other, remote brain regions. We employed
523 searchlight MVPA, moving a spherical region-of-interest (or “searchlight”) of 5 mm radius
524 through the entire brain (Kriegeskorte et al., 2006). At each searchlight location, a machine-
525 learning classifier (an L2-norm support vector machine; $C=1$) aimed to decode between effective
526 and sham TMS, separately for words and pseudowords. We used leave-one-*participant*-out cross
527 validation (CV), training on the activation patterns from $n-1$ participants and testing on the left-
528 out participant (yielding 28 CV-folds). For statistical inference, we performed a permutation test
529 across the accuracy-minus-chance maps of the different CV-folds (using *SnPM13*; as proposed by
530 Wang et al., 2021), thresholded at a voxel-wise $p < 0.001$ and a cluster-wise $p < 0.05$ FWE-
531 corrected (as in our univariate analyses). Activity patterns comprised beta estimates for each mini-
532 block of every participant.

533 ***Dynamic Causal Modelling (DCM)***

534 Finally, we performed dynamic causal modelling (DCM; Friston et al., 2003) to investigate TMS-
535 induced changes in effective connectivity (i.e., directed causal influences) between the core nodes
536 of the reading network. DCM estimates a model of effective connectivity between brain regions
537 to predict a neuroimaging time series. A DCM consists of three types of parameters: 1) “intrinsic”
538 (i.e., condition-independent) directed connections between brain regions, 2) “modulatory inputs”
539 that change connection strengths during a certain experimental manipulation, and 3) “driving
540 inputs” that drive activity in the network. The goal of DCM is to optimize a tradeoff between
541 model fit (of the predicted to observed time series) and complexity (i.e., deviation of model
542 parameters from their prior expectations), measured by the model evidence (Kahan & Foltynie,
543 2013; Zeidman et al., 2019a).

544 We performed a two-level analysis using Parametric Empirical Bayes (PEB) and Bayesian
545 Model Reduction (BMR)—the current “standard practice for group DCM studies” (Friston et al.,
546 2016). At the first level, a “full model” was specified and estimated for each participant (see
547 Results section). Regions included in the model were the left TPC (the stimulated region), left
548 vOTC, and left IFG. The three regions were defined functionally in each individual participant as
549 the top 10% most activated voxels for [all sham trials > rest] within 20 mm spheres around the
550 MNI peak coordinates in a meta-analysis of reading in adults (Martin et al., 2015): left TPC = -49
551 -44 21; left IFG = -52 20 18; left vOTC = -42 -68 -22. All regions were restricted to the cerebral
552 gray matter. The first eigenvariate of the BOLD time series of each region was extracted and
553 adjusted for effects-of-interest (all experimental conditions) using our participant-level GLM (see
554 Univariate analyses). DCM inputs were mean-centered, so that the intrinsic connections reflected
555 the mean connectivity across experimental conditions (Zeidman et al., 2019a).

556 At the second level, DCM parameters of individual participants were entered into a GLM—
557 the PEB model—that decomposed interindividual variability in connection strengths into group
558 effects and random effects (Zeidman et al., 2019b). BMR then compared the full model against
559 numerous reduced models that had certain parameters “switched off” (i.e., prior mean and variance
560 set to 0) (Friston et al., 2016). Finally, we computed the Bayesian model average (BMA), the
561 average of parameter values across models weighted by each model’s posterior probability (Pp)
562 (Penny et al., 2007). This approach is preferred over exclusively assessing the parameters of the
563 “best” model as it accommodates uncertainty about the true underlying model (Friston et al., 2016;
564 Dijkstra et al., 2017). The BMA was thresholded to only retain parameters with a Pp > 99% (cf.
565 Zeidman et al., 2019b; Kuhnke et al., 2021). For each modulatory input, we calculated the resulting
566 connectivity value (in Hz) using formula 3 in Zeidman et al. (2019a). Finally, to determine whether
567 one experimental condition modulated a certain connection more strongly than another, we directly
568 compared different parameters on the same connection using Bayesian contrasts (Dijkstra et al.,
569 2017; Kuhnke et al., 2021).

570 **6. Acknowledgements**

571 The present work was supported by the Max Planck Society and the Humboldt Foundation.

572 **7. Competing interests**

573 The authors declare no competing financial or nonfinancial interests.

574 **8. Bibliography**

575 Barr, D. & Levy, R., Scheepers, C. & Tily, H. J. (2013). Random effects structure for confirmatory
576 hypothesis testing: Keep it maximal. *Journal of Memory and Language*, 68(3). 255-278.
577 <https://doi.org/10.1016/j.jml.2012.11.001>

578 Bergmann TO, Hartwigsen G. Inferring Causality from Noninvasive Brain Stimulation in
579 Cognitive Neuroscience. *Journal of Cognitive Neuroscience* 33(2), 195-225. doi:
580 10.1162/jocn_a_01591.

581 Binder, J. R., Westbury, C. F., McKiernan, K. A., Possing, E. T. & Medler, D. A. (2005). Distinct
582 brain systems for processing concrete and abstract concepts. *Journal of Cognitive*
583 *Neuroscience*, 17(6), 905-917. 10.1162/0898929054021102

584 Brooks, M. E., Kristensen, K., van Benthem, K. J., Magnusson, A., Berg, C. W., Nielsen, A.,
585 Skaug, H. J., Maechler, M. & Bolker, B. M. (2017). GlmmTMB balances speed and
586 flexibility among packages for zero-inflated generalized linear mixed modeling. *The R*
587 *Journal*, 9(2), 378–400. <https://doi.org/10.32614/RJ-2017-066>

588 Brown, S., Ingham, R. J., Ingham, J. C., Laird, A. R., & Fox, P. T. (2005). Stuttered and fluent
589 speech production: An ALE meta-analysis of functional neuroimaging studies. *Human*
590 *Brain Mapping*, 25(1), 105–117. <https://doi.org/10.1002/hbm.20140>

591 Brozdowski, C. & Booth, J. (2021). Reading skill correlates in frontal cortex during semantic and
592 phonological processing. *PsyArXiv*. 10.31234/osf.io/d3mj7

593 Behzadi, Y., Restom, K., Liao, J., & Liu, T. T. (2007). A component based noise correction method
594 (CompCor) for BOLD and perfusion based fMRI. *NeuroImage*, 37(1), 90–101.
595 <https://doi.org/10.1016/j.neuroimage.2007.04.042>

596 Chyl, K., Fraga González, G., Brem, S. & Jednoróg, K. (2021). Brain dynamics of (a)typical
597 reading development: A review of longitudinal studies. *npj Science of Learning*,
598 6(1), 1-9. <https://doi.org/10.1038/s41539-020-00081-5>

599 Coltheart, M., Rastle, K., Perry, C., Langdon, R., & Ziegler, J. (2001). DRC: A dual route cascaded
600 model of visual word recognition and reading aloud. *Psychological Review*, 108(1),
601 204- 256. <https://doi.org/10.1037/0033-295X.108.1.fpeter204>

- 602 Corbetta, M., & Shulman, G. L. (2002). Control of goal-directed and stimulus-driven attention in
603 the brain. *Nature reviews Neuroscience*, 3(3), 201–215. <https://doi.org/10.1038/nrn755>
- 604 Costanzo, F., Menghini, D., Caltagirone, C. & Oliveri, M. (2012). High frequency rTMS over the
605 left parietal lobule increases non-word reading accuracy. *Neuropsychologia*,
606 50(11), 2645- 2651. <https://doi.org/10.1016/j.neuropsychologia.2012.07.017>
- 607 Costanzo, F., Varuzza, C., Rossi, S., Sdoia, S., Varvara, P., Oliveri, M., Giacomo, K., Vicari, S.
608 & Menghini, D. (2016). Evidence for reading improvement following tDCS treatment in
609 children and adolescents with dyslexia. *Restorative Neurology and Neuroscience*, 34(2),
610 215–226. 10.3233/RNN-150561
- 611 Costanzo, F., Rossi, S., Varuzza, C., Varvara, P., Vicari, S. & Menghini, D. (2019). Long-lasting
612 improvement following tDCS treatment combined with a training for reading in children
613 and adolescents with dyslexia. *Neuropsychologia*, 130, 38–43.
614 <https://doi.org/10.1016/j.neuropsychologia.2018.03.016>
- 615 Cummine, J., Dai, W., Borowsky, R., Gould, L., Rollans, C., & Boliek, C. (2015). Investigating
616 the ventral-lexical, dorsal-sublexical model of basic reading processes using diffusion
617 tensor imaging. *Brain Structure and Function*, 220(1), 445-455.
618 <https://doi.org/10.1007/s00429-013-0666-8>
- 619 Devlin, J. T., Matthews, P. M. & Rushworth, M. F. (2003). Semantic
620 processing in the left inferior prefrontal cortex: A combined
621 functional magnetic resonance imaging and transcranial
622 magnetic stimulation study. *Journal of Cognitive Neuroscience*, 15(1), 71–84.
623 <https://doi.org/10.1162/089892903321107837>
- 624 Dijkstra, N., Zeidman, P., Ondobaka, S., van Gerven, M., & Friston, K. (2017). Distinct top-down
625 and bottom-up brain connectivity during visual perception and imagery. *Scientific*
626 *Reports*, 7(1), Article 5677. <https://doi.org/10.1038/s41598-017-05888-8>
- 627 Duncan, K. J., Pattamadilok, C., & Devlin, J. T. (2010). Investigating occipito-temporal
628 contributions to reading with TMS. *Journal of Cognitive Neuroscience*, 22(4), 739–750.
629 <https://doi.org/10.1162/jocn.2009.21207>
- 630 Ehri, L. C. (2005). Development of Sight Word Reading: Phases and Findings. In M. J. Snowling
631 & C. Hulme (Eds.), *The science of reading: A handbook* (pp. 135–154). Blackwell
632 Publishing. <https://doi.org/10.1002/9780470757642.ch8>

- 633 Esteban, O., Markiewicz, C. J., Blair, R. W., Moodie, C. A., Isik, A. I., Erramuzpe, A., Kent, J.
634 D., Goncalves, M., DuPre, E., Snyder, M., Oya, H., Ghosh, S. S., Wright, J., Durnez, J.,
635 Poldrack, R. A., & Gorgolewski, K. J. (2019). fMRIPrep: A robust preprocessing pipeline
636 for functional MRI. *Nature methods*, *16*(1), 111–116. [https://doi.org/10.1038/s41592-018-](https://doi.org/10.1038/s41592-018-0235-4)
637 [0235-4](https://doi.org/10.1038/s41592-018-0235-4)
- 638 Friston, K. J., Harrison, L., & Penny, W. (2003). Dynamic causal modelling. *NeuroImage*, *19*(4),
639 1273–1302. [https://doi.org/10.1016/s1053-8119\(03\)00202-7](https://doi.org/10.1016/s1053-8119(03)00202-7)
- 640 Friston, K., Brown, H. R., Siemerkus, J., & Stephan, K. E. (2016). The dysconnection
641 hypothesis. *Schizophrenia Research*, *176*(2-3), 83–
642 94. <https://doi.org/10.1016/j.schres.2016.07.014>
- 643 Gagl, B., Sassenhagen, J., Haan, S., Gregorova, K., Richlan, F., & Fiebach, C. J. (2020). An
644 orthographic prediction error as the basis for efficient visual word
645 recognition. *NeuroImage*, *214*, 116727.
646 <https://doi.org/10.1016/j.neuroimage.2020.116727>
- 647 Gough, P. M., Nobre, A. C. & Devlin, J. T. (2005). Dissociating linguistic processes in the left
648 inferior frontal cortex with transcranial magnetic stimulation. *Journal of Neuroscience*
649 *25*(35), 8010–8016. <https://doi.org/10.1523/JNEUROSCI.2307-05.2005>
- 650 Hallam, G. P., Whitney, C.; Hymers, M., Gouws, A. D. & Jefferies, E. (2016). Charting the effects
651 of TMS with fMRI: Modulation of cortical recruitment within the distributed network
652 supporting semantic control. *Neuropsychologia*, *93*, 40-52.
653 <https://doi.org/10.1016/j.neuropsychologia.2016.09.012>
- 654 Hamada, M., Murase, N., Hasan, A., Balaratnam, M., & Rothwell, J. C. (2013). The role of
655 interneuron networks in driving human motor cortical plasticity. *Cerebral Cortex*, *23*(7),
656 1593–1605. <https://doi.org/10.1093/cercor/bhs147>
- 657 Hartwigsen, G. (2016). Adaptive plasticity in the healthy language network: Implications for
658 language recovery after stroke. *Neural Plasticity*, *2016*, 1–18.
659 <https://doi.org/10.1155/2016/9674790>
- 660 Hartwigsen G. (2018). Flexible Redistribution in cognitive networks. *Trends in Cognitive*
661 *Sciences*, *22*(8), 687–698. <https://doi.org/10.1016/j.tics.2018.05.008>
- 662 Hartwigsen, G., & Volz, L. J. (2021). Probing rapid network reorganization of motor and language
663 functions via neuromodulation and neuroimaging. *NeuroImage*, *224*, Article 117449.

- 664 <https://doi.org/10.1016/j.neuroimage.2020.117449>
- 665 Hartwigsen, G., Price, C., Baumgaertner, A., Geiss, G., Koehnke, M., Ulmer, S. & Siebner, H. R.
666 (2010a). The right posterior inferior frontal gyrus contributes to phonological word
667 decisions in the healthy brain: Evidence from dual-site TMS. *Neuropsychologia*, *48*(10),
668 3155-3163. <https://doi.org/10.1016/j.neuropsychologia.2010.06.032>
- 669 Hartwigsen G, Baumgaertner A, Price, C. J., Koehnke, M., Ulmer, S. & Siebner, H. R. (2010b).
670 Phonological decisions require both the left and right supramarginal gyri. *PNAS*, *107*(38),
671 16494–16499. <https://doi.org/10.1073/pnas.1008121107>
- 672 Hartwigsen, G., Saur, D., Price, C. J., Ulmer, S., Baumgaertner, A., & Siebner, H. R. (2013).
673 Perturbation of the left inferior frontal gyrus triggers adaptive plasticity in the right
674 homologous area during speech production. *PNAS*, *110*(41), 16402-16407.
675 <https://doi.org/10.1073/pnas.1310190110>
- 676 Hartwigsen, G., Bzdok, D., Klein, M., Wawrzyniak, M., Stockert, A., Wrede, K., Classen, J. &
677 Saur, D. (2017). Rapid short-term reorganization in the language network. *ELife*, *6*.
678 10.7554/eLife.25964
- 679 Hauck, T., Tanigawa, N., Probst, M., Wohlschlaeger, A., Ille, S., Sollmann, N., Maurer, S.,
680 Zimmer, C., Ringel, F., Meyer, B. & Krieg, S. M. (2015a). Stimulation frequency
681 determines the distribution of language positive cortical regions during navigated
682 transcranial magnetic brain stimulation. *BMC Neuroscience*, *16*(5), 1-14. 10.1186/s12868-
683 015-0143-9
- 684 Hauck, T., Tanigawa, N., Probst, M., Wohlschlaeger, A., Ille, S., Sollmann, N., Maurer, S.,
685 Zimmer, C., Ringel, F., Meyer, B. & Krieg, S. M. (2015b). Task type affects location of
686 language: Positive cortical regions by repetitive navigated transcranial magnetic
687 stimulation mapping. *PLOS One*, *10*(4), 1-21.
688 <https://doi.org/10.1371/journal.pone.0125298>
- 689 Haxby, J. V., Connolly, A. C. & Swaroop Guntupalli, J. (2014). Decoding neural
690 representational spaces using multivariate pattern analysis. *Annual Review of*
691 *Neuroscience*, *37*(1), 435-456. <https://doi.org/10.1146/annurev-neuro-062012-170325>
- 692 Hebart, M. N., Gorgen, K., & Haynes, J. D. (2015). The Decoding Toolbox (TDT): A versatile
693 software package for multivariate analyses of functional imaging data. *Frontiers in*
694 *Neuroinformatics*, *8*(88). <https://doi.org/10.3389/fninf.2014.00088>

- 695 Huang, Y. Z., Edwards, M. J., Rounis, E., Bhatia, K. P., & Rothwell, J. C. (2005). Theta burst
696 stimulation of the human motor cortex. *Neuron*, 45(2), 201-206.
697 <https://doi.org/10.1016/j.neuron.2004.12.033>
- 698 Jobard, G., Crivello, F. & Tzourio-Mazoyer, N. (2003). Evaluation of the dual route theory of
699 reading: A metaanalysis of 35 neuroimaging studies. *Neuroimage*, 20(2), 693-712.
700 [https://doi.org/10.1016/S1053-8119\(03\)00343-4](https://doi.org/10.1016/S1053-8119(03)00343-4)
- 701 Jonides, J., Smith, E., Marshuetz, C., Koeppe, R., & Reuter-Lorenz, P. (1998). Inhibition in verbal
702 working memory revealed by brain activity. *PNAS*, 95(14), 8410-8413.
703 <https://doi.org/10.1073/pnas.95.14.8410>
- 704 Jung, J. Y. & Lambon Ralph, M. A. (2016). Mapping the dynamic network interactions
705 underpinning cognition: A cTBS-fMRI study of the flexible adaptive neural system for
706 semantics. *Cerebral Cortex*, 26(8), 3580–3590. [10.1093/cercor/bhw149](https://doi.org/10.1093/cercor/bhw149)
- 707 Kahan, J., & Foltynie, T. (2013). Understanding DCM: ten simple rules for the
708 clinician. *NeuroImage*, 83, 542–549. <https://doi.org/10.1016/j.neuroimage.2013.07.008>
- 709 Kriegeskorte, N., Goebel, R. & Bandettini, P. (2006). Information-based functional brainmapping.
710 *PNAS*, 103(10), 3863–3868. <https://doi.org/10.1073/pnas.0600244103>
- 711 Kuhnke, P., Beaupain, M. C., Cheung, V. K. M., Weise, K., Kiefer, M., & Hartwigsen, G. (2020).
712 Left posterior inferior parietal cortex causally supports the retrieval of action knowledge.
713 *Neuroimage*, 219, Article 117041. <https://doi.org/10.1016/j.neuroimage.2020.117041>
- 714 Kuhnke, P., Kiefer, M. & Hartwigsen, G. (2021). Task-Dependent Functional and Effective
715 Connectivity during Conceptual Processing. *Cerebral Cortex*, 31(7), 3475–
716 3493. <https://doi.org/10.1093/cercor/bhab026>
- 717 Lazzaro, G., Costanzo, F., Varuzza, C., Rossi, S., Matteis, M. & Menghini, D. (2020). Individual
718 differences modulate the effects of tDCS on reading in children and adolescents with
719 dyslexia. *Scientific Studies of Reading*, 25(6), 470-485.
720 <https://doi.org/10.1080/10888438.2020.1842413>
- 721 Lazzaro, G., Bertoni, S., Menghini, D., Costanzo, F., Franceschini, S., Varuzza, C., Ronconi, L.,
722 Battisti, A., Gori, S., Facoetti, A., & Vicari, S. (2021). Beyond reading modulation:
723 Temporo-parietal tdcS alters visuo-spatial attention and motion perception in
724 dyslexia. *Brain Sciences*, 11(2), 1-17. <https://doi.org/10.3390/brainsci11020263>

- 725 Liederman, J., McGraw Fischer, J. & Schulz, M. (2003). The role of motion direction selective
726 extrastriate regions in reading: A transcranial magnetic stimulation study. *Brain and*
727 *Language*, 85(1): 140-155. [https://doi.org/10.1016/S0093-934X\(02\)00550-3](https://doi.org/10.1016/S0093-934X(02)00550-3)
- 728 Petermann, F. & Daseking, M. (2019). Zürcher Lesetest – II: Weiterentwicklung des Zürcher
729 Lesetests (ZLT) von Maria Linder und Hans Grisseemann. Göttingen, Germany: Hogrefe.
- 730 Linkersdörfer, J., Lonnemann, J., Lindberg, S., Hasselhorn, M. & Fiebach, C. J. (2012). Grey
731 matter alterations co-localize with functional abnormalities in developmental dyslexia: An
732 ALE meta-analysis. *PLOS One*, 7(8), 1–10. <https://doi.org/10.1371/journal.pone.0043122>
- 733 Lo, S. & Andrews. S. (2015). To transform or not to transform: using generalized linear mixed
734 models to analyse reaction time data. *Frontiers in Psychology*, 6, Article 1171.
735 [10.3389/fpsyg.2015.01171](https://doi.org/10.3389/fpsyg.2015.01171)
- 736 Luber, B., & Lisanby, S. H. (2014). Enhancement of human cognitive performance using
737 transcranial magnetic stimulation (TMS). *Neuroimage*, 85, 961–970. DOI:
738 <https://doi.org/10.1016/j.neuroimage.2013.06.007>.
- 739 Maisog, J. M., Einbinder, E. R., Flowers, D. L., Turkeltaub, P. E., & Eden, G. F. (2008). A meta-
740 analysis of functional neuroimaging studies of dyslexia. *Annals of the New York Academy*
741 *of Sciences*, 1145(1), 237-259.
- 742 Martin, A., Schurz, M., Kronbichler, M., & Richlan, F. (2015). Reading in the brain of children
743 and adults: A meta-analysis of 40 functional magnetic resonance imaging studies. *Human*
744 *Brain Mapping*, 36(5), 1963–1981. <https://doi.org/10.1002/hbm.22749>
- 745 Miniussi, C., Harris, J. A., & Ruzzoli, M. (2013). Modelling non-invasive brain stimulation in
746 cognitive neuroscience. *Neuroscience and Biobehavioral Reviews*, 37(8), 1702–1712.
747 <https://doi.org/10.1016/j.neubiorev.2013.06.014>
- 748 Moll, K. & Landerl, K. (2014). SLRT-II: Lese- und Rechtschreibtest – Weiterentwicklung des
749 Salzburger Lese- und Rechtschreibtests (SLRT). Bern, Switzerland: Huber.
- 750 Pattamadilok, C., Bulnes, L. C., Devlin, J. T., Bourguignon, M., Morais, J., Goldman, S. &
751 Kolinsky, R. (2015). How early does the brain distinguish between regular words, irregular
752 words, and pseudowords during the reading process? Evidence from neurochronometric
753 TMS. *Journal of Cognitive Neuroscience*, 27(6), 1259-1274.
754 https://doi.org/10.1162/jocn_a_00779
- 755 Penny, W., Flandin, G. & Trujillo-Barreto, N. (2007). Bayesian comparison of spatially

- 756 regularised general linear models. *Human Brain Mapping*, 28(4), 275-93.
757 0.1002/hbm.20327
- 758 Petermann, F. & Petermann, U. (2011). WISC-IV. Wechsler Intelligence Scale for Children–
759 Fourth Edition. Frankfurt, Germany: Pearson.
- 760 Pugh, K. R., Mencl, W. E., Jenner, A. R., Katz, L., Frost, S. J., Lee, J. R., Shawitz, S. E. &
761 Shaywitz, B. A. (2001). Neurobiological studies of reading and reading disability. *Journal*
762 *of Communication Disorders*, 32, 479–492.
763 [https://doi.org/10.1016/S00219924\(01\)00060-0](https://doi.org/10.1016/S00219924(01)00060-0)
- 764 Taylor, J. S., Rastle, K., & Davis, M. H. (2013). Can cognitive models explain brain activation
765 during word and pseudoword reading? A meta-analysis of 36 neuroimaging
766 studies. *Psychological Bulletin*, 139(4), 766–791. <https://doi.org/10.1037/a0030266>
- 767 Richlan, F., Kronbichler, M., & Wimmer, H. (2009). Functional abnormalities in the dyslexic
768 brain: A quantitative meta-analysis of neuroimaging studies. *Human brain mapping*,
769 30(10), 3299-3308. <https://doi.org/10.1002/hbm.20752>
- 770 Richlan, F., Kronbichler, M., & Wimmer, H. (2011). Meta-analyzing brain dysfunctions in
771 dyslexic children and adults. *NeuroImage*, 56(3), 1735–1742.
772 <https://doi.org/10.1016/j.neuroimage.2011.02.040>
- 773 Richlan, F., Kronbichler, M., & Wimmer, H. (2013). Structural abnormalities in the dyslexic brain:
774 A meta-analysis of voxel-based morphometry studies. *Human Brain Mapping*, 34(11),
775 3055–3065. <https://doi.org/10.1002/hbm.22127>
- 776 Rueckl, J. G., Paz-Alonso, P. M., Molfese, P. J., Kuo, W. J., Bick, A., Frost, S. J., ... & Frost, R.
777 (2015). Universal brain signature of proficient reading: Evidence from four contrasting
778 languages. *Proceedings of the National Academy of Sciences*, 112(50), 15510-15515.
779 <https://doi.org/10.1073/pnas.1509321112>
- 780 Sale, M. V., Mattingley, J. B., Zalesky, A. & Cocchi, L. (2015). Imaging human brain networks to
781 improve the clinical efficacy of non-invasive brain stimulation. *Neuroscience and*
782 *Biobehavioral Reviews*, 57, 187-198. <https://doi.org/10.1016/j.neubiorev.2015.09.010>
- 783 Schneider, W., Schlagmüller, M., Ennemoser, M. (2017). Lesegeschwindigkeits- und
784 Verständnistest für die Klassen 5-12+. Göttingen, Germany: Hogrefe.

- 785 Schurz, M., Wimmer, H., Richlan, F., Ludersdorfer, P., Klackl, J., & Kronbichler, M. (2015).
786 Resting-State and task-based functional brain connectivity in developmental
787 dyslexia. *Cerebral Cortex*, 25(10), 3502–3514. <https://doi.org/10.1093/cercor/bhu184>
- 788 Schuster, S., Hawelka, S., Richlan, F., Ludersdorfer, P., & Hutzler, F. (2015). Eyes on words: A
789 fixation-related fMRI study of the left occipito-temporal cortex during self-paced silent
790 reading of words and pseudowords. *Scientific reports*, 5(1), 1-11.
791 <https://doi.org/10.1038/srep12686>
- 792 Schutter, D. J., & van Honk, J. (2006). An electrophysiological link between the cerebellum,
793 cognition and emotion: Frontal theta EEG activity to single-pulse cerebellar
794 TMS. *NeuroImage*, 33(4), 1227–1231. <https://doi.org/10.1016/j.neuroimage.2006.06.055>
- 795 Seidenberg, M. S. (2005). Connectionist models of word reading. *Current Directions in*
796 *Psychological Science*, 14(5), 238-242. <https://doi.org/10.1111/j.09637214.2005.00372.x>.
- 797 Siebner, H. R. & Rothwell, J. (2003). Transcranial magnetic stimulation: New insights into
798 representational cortical plasticity. *Experimental Brain Research*, 148(1), 1–16.
799 <https://doi.org/10.1007/s00221-002-1234-2>
- 800 Siegel, J., Power, J., Dubis, J., Vogel, A., Church, J., Schlaggar, B. & Petersen, S. (2014).
801 Statistical improvements in functional magnetic resonance imaging analyses produced
802 by censoring high-motion data points. *Human Brain Mapping*, 35(5), 1981-1996.
803 [10.1002/hbm.22307](https://doi.org/10.1002/hbm.22307)
- 804 Smallwood, J., Bernhardt, B. C., Leech, R., Bzdok, D., Jefferies, E. & Margulies, D. S., (2021).
805 The default mode network in cognition: a topographical perspective. *Nature Reviews*
806 *Neuroscience*, 22, 503-513. [10.1038/s41583-021-00474-4](https://doi.org/10.1038/s41583-021-00474-4)
- 807 Tops, M., & Boksem, M. A. (2011). A potential role of the inferior frontal gyrus and anterior insula
808 in cognitive control, brain rhythms, and event-related potentials. *Frontiers in*
809 *Psychology*, 2, Article 330. <https://doi.org/10.3389/fpsyg.2011.00330>
- 810 Turker, S. (2018). Exploring the neurofunctional underpinnings of developmental dyslexia: A
811 review focussing on dyslexic children. In E. Luef & M. Marin (Eds.), *The talking*
812 *species* (p. 495). Uni Graz Press.
- 813 Turker, S., & Hartwigsen, G. (2021a). Exploring the neurobiology of reading through non-invasive
814 brain stimulation: A review. *Cortex*. 141, 497–521.
815 <https://doi.org/10.1016/j.cortex.2021.05.001>

- 816 Turker, S., & Hartwigsen, G. (2021b). The use of noninvasive brain stimulation techniques to
817 improve reading difficulties in dyslexia: A systematic review. *Human Brain Mapping*.
818 43(3), 1157-1173. <https://doi.org/10.1002/hbm.25700>
- 819 van der Mark, S., Klaver, P., Bucher, K., Maurer, U., Schulz, E., Brem, S., Martin, E., & Brandeis,
820 D. (2011). The left occipitotemporal system in reading: Disruption of focal fMRI
821 connectivity to left inferior frontal and inferior parietal language areas in children with
822 dyslexia. *NeuroImage*, 54(3), 2426–2436.
823 <https://doi.org/10.1016/j.neuroimage.2010.10.002>
- 824 Wang, Q., Akram, H., Muthuraman, M., Gonzalez-Escamilla, G., Sheth, S. A., Oxenford, S., Yeh,
825 F. C., Groppa, S., Vanegas-Arroyave, N., Zrinzo, L., Li, N., Kühn, A., & Horn, A. (2021).
826 Normative vs. patient-specific brain connectivity in deep brain
827 stimulation. *NeuroImage*, 224, Article 117307.
828 <https://doi.org/10.1016/j.neuroimage.2020.117307>
- 829 Weiß, R. (2019). Grundintelligenztest Skala 2 – Revision (CFT 20-R) mit Wortschatztest (WS)
830 und Zahlenfolgentest (ZF) – Revision (WS/ZF-R). Göttingen, Germany: Hogrefe.
- 831 Xia, Z., Hancock, R., & Hoeft, F. (2017). Neurobiological bases of reading disorder Part I:
832 Etiological investigations. *Language And Linguistics Compass*, 11(4).
833 <https://doi.org/10.1111/lnc3.12239>
- 834 Zeidman, P., Jafarian, A., Corbin, N., Seghier, M., Razi, A., Price, C. & Friston, K.. (2019a). A
835 guide to group effective connectivity analysis, part 1: First level analysis with DCM for
836 fMRI. *NeuroImage*, 200, 174-190. <https://doi.org/10.1016/j.neuroimage.2019.06.031>
- 837 Zeidman, P., Amirhossein, J., Seghier, M. L., Litvak, V., Cagnan, H., Price, C. J. & Friston, K. J.
838 (2019b). A guide to group effective connectivity analysis, part 2: Second level analysis
839 with PEB. *NeuroImage*, 200, 12-25. <https://doi.org/10.1016/j.neuroimage.2019.06.032>